

On optimal three-impulse Earth-Moon transfers in a four-body model

Shanshan Pan¹, Francesco Topputo², Xiyun Hou³, Yang Wang⁴,

Optimization of three-impulse, low-energy Earth-Moon transfer trajectories with a fixed time of flight in the restricted four-body problem is investigated in this work. Based on the two-impulse, low-energy solutions, a strategy is developed to design the time-fixed optimal three-impulse Earth-Moon transfers. The necessary conditions of optimality for a two-impulse transfer are stated in terms of the primer vector. Primer vector theory is then extended to nonoptimal two-impulse trajectories to establish a criterion whereby adding an interior impulse reduces total fuel expenditure. Examples of optimal three-impulse, low-energy Earth-Moon transfer trajectories are presented. The differences between the two-impulse transfers and three-impulse transfers are discussed.

1 Introduction

The Earth-Moon transfer trajectory of a spacecraft has been studied extensively in the past years. The traditional way to construct a direct transfer trajectory from the Earth to the Moon is the Hohmann transfer in the two-body problem, which considers the transfer between two concentric circles with two impulses. However, the Hohmann transfer usually requires a high fuel cost and hardly meets the always-increasing demand for science-to-investment ratios in future space missions. Therefore, low-energy transfers in the multi-body models, such as the circular restricted three-body problem (CRTBP) and bicircular restricted four-body problem (BRFBP), have been introduced to design the low-energy Earth-Moon transfers [1–12]. Compared to the Hohmann transfer, the low-energy transfers to the Moon are appealing due to the lower fuel cost, and more flexible launch window options [12–15]. Low-energy transfers have been applied successfully to missions including: the *Hiten* mission [16, 17], the *Genesis* mission [18], and the GRIAL mission [14, 19, 20].

The approach of two-impulse transfers from the Earth to the Moon is the most widely studied transfer in previous works. Topputo [12] and Oshima [15] constructed the global set of solutions for the two-impulse, low-energy transfers to the Moon within 100 days and 200 days, respectively. They found that many of the

known solutions are local optimal solutions of a more general picture. However, fewer results have been obtained for the three-impulse transfers to the Moon. In addition to increasing the transfer time, will the fuel consumption be further reduced by adding an additional impulse? In the present paper, we extend the work in Topputo [12] to compute the optimal three-impulse, low-energy transfers to the Moon.

The trajectory optimization method used in this work is based on the primer vector theory. The primer vector theory was first introduced by Lawden [21], which is a byproduct of applying the Calculus of Variations (COV) to the problem of minimizing the fuel consumption of impulsive trajectories. The necessary conditions for the fuel optimality of impulsive trajectories were derived by Lawden using the primer vector. After that, numerous contributions emerged in the field of trajectory optimization using the primer vector theory [22–31]. The definition of the primer vector was first extended to nonoptimal impulsive trajectories by Lion and Handelsman [22]. They indicated that a nonoptimal trajectory can be improved by adding an additional mid-course impulse or terminal coasts. The method of applying the primer vector theory to obtain the multi-impulse solutions was developed by Jezewski and Rozendaal [23]. Additionally, utilizing a second-order approximation for the cost function J , Jezewski and Rozendaal provided an estimate for the impulse magnitude which provides a maximum improvement in J . In this work, we mainly focus on time-fixed trajectories optimization. Primer vector theory applied to time-fixed trajectories optimization in an inverse-square gravitational field have employed by several searchers [24–27, 32–36], concerning the rendezvous and interception problem with path constraints. Besides, D’Amario and Edelbaum [37] applied primer vector theory to construct and optimize time-fixed transfer trajectories in the restricted three-body problem. The strategy using primer vector theory to de-

¹Ph.D. Candidate, School of Astronomy and Space Science, Nanjing University, 163 Xianlin Ave, Qixia District, Nanjing 210023, China, pshanshan@smail.nju.edu.cn

²Full Professor, Department of Aerospace Science and Technology, Politecnico di Milano, Via La Masa 34, 20156, Milan, Italy, francesco.topputo@polimi.it

³Full Professor, School of Astronomy and Space Science, Nanjing University, 163 Xianlin Ave, Qixia District, Nanjing 210023, China, houxiyun@nju.edu.cn

⁴Ph.D., Department of Aerospace Science and Technology, Politecnico di Milano, Via La Masa 34, 20156, Milan, Italy, yang.wang@polimi.it

sign optimal time-fixed impulsive transfers was extended to the elliptic restricted three-body problem by Hiday [28, 29] to solve the transfer problem between libration point orbits.

The objective of this study includes the determination of three-impulse transfers from Earth to the Moon in the planar bicircular restricted four-body problem. In addition, since fuel savings are highly desirable in mission design, exploration of the optimality of a transfer trajectory is of utmost importance. Here, the optimum is defined to be minimum characteristic velocity or, equivalently, minimum of the sum of impulsive maneuvers. The transfer duration is given by the optimal two-impulse solutions and is fixed. Therefore, the allowance for coastal arcs in the initial and final orbits is not considered here. Only the addition of interior impulse is examined as a means of minimizing total fuel expenditure.

The remainder of the paper is structured as follows. In Sect. 2, the model framework is introduced, including the planar bicircular restricted four-body problem and the primer vector theory. The optimization problem statement is given in Sect. 3. In Sect. 4, the methodology of generating the optimal three-impulse solutions is depicted. Specific results are presented and discussed in Sect. 5. The conclusion is given in Sect. 6.

2 Dynamics

2.1 Planar Bicircular Restricted Four-Body Problem

In the Planar Bicircular Restricted Four-Body Problem (PBRFBP), a massless particle, P , moves in the gravitational field generated by the three massive primaries, P_0 , P_1 and P_2 of masses $m_0 > m_1 > m_2 > 0$, respectively. It is assumed that the two primaries (P_1 and P_2) have circular orbits about their common center of mass due to their mutual gravitational attraction and P_0 revolves in a circular orbit around the barycenter of P_1 and P_2 . The four bodies P_0 , P_1 , P_2 and P move in the same plane. In this work, P_0 , P_1 , and P_2 represent the Sun, the Earth, and the Moon, respectively. Usually, dynamics of the PBRFBP model are formulated in a rotating frame (synodic frame) with non-dimensional units. The state vector of the spacecraft P is defined as

$$\mathbf{x} = \begin{bmatrix} \mathbf{r} \\ \mathbf{v} \end{bmatrix} \quad (1)$$

where \mathbf{r} , \mathbf{v} are the position and velocity vector of P , respectively. The equations of motion in the PBRFBP model are [38, 39]

$$\dot{\mathbf{x}} = f(\mathbf{x}, t) \quad (2)$$

$$\begin{bmatrix} \dot{\mathbf{r}} \\ \dot{\mathbf{v}} \end{bmatrix} = \begin{bmatrix} \mathbf{v} \\ \mathbf{g}(\mathbf{r}, \mathbf{v}, t) \end{bmatrix} \quad (3)$$

where t is the non-dimensional time, $\mathbf{g}(\mathbf{r}, \mathbf{v}, t)$ is defined as follows:

$$\mathbf{g}(\mathbf{r}, \mathbf{v}, t) = \begin{bmatrix} 2\dot{y} + \frac{\partial \Omega_4}{\partial x} \\ -2\dot{x} + \frac{\partial \Omega_4}{\partial y} \end{bmatrix} \quad (4)$$

in which Ω_4 is the gravitational potential in the PBRFBP model, reads

$$\Omega_4(x, y) = \Omega_3(x, y) + \frac{m_s}{r_3(t)} - \frac{m_s}{\rho^2} (x \cos \omega_s t + y \sin \omega_s t) \quad (5)$$

$$\Omega_3 = \frac{1}{2} [(x^2 + y^2) + \mu(1 - \mu)] + \frac{1 - \mu}{r_1} + \frac{\mu}{r_2} \quad (6)$$

In Eq. (5), m_s is the mass of the Sun, ρ is the distance between the Sun and the Earth-Moon barycenter, ω_s is the angular velocity of the Sun in the Earth-Moon rotating frame, and r_3 is the distance between the Sun and the spacecraft, defined as

$$r_3(t) = [(x - \rho \cos(\omega_s t))^2 + (y - \rho \sin(\omega_s t))^2]^{1/2} \quad (7)$$

All physical parameters used in this paper are consistent with those in Table 3 of [12].

2.2 Primer Vector Theory

For coast arcs, i.e., null thrust arcs (NT arcs), Eq. (3) can be linearized [40]. The variational state equations take the form

$$\begin{bmatrix} \delta \dot{\mathbf{r}} \\ \delta \dot{\mathbf{v}} \end{bmatrix} = \begin{bmatrix} 0 & I \\ \mathbf{G}_r & \mathbf{G}_v \end{bmatrix} \begin{bmatrix} \delta \mathbf{r} \\ \delta \mathbf{v} \end{bmatrix} \quad (8)$$

in which

$$\mathbf{G}_r = \begin{bmatrix} \Omega_{4xx} & \Omega_{4xy} \\ \Omega_{4yx} & \Omega_{4yy} \end{bmatrix} \quad \mathbf{G}_v = \begin{bmatrix} 0 & 2 \\ -2 & 0 \end{bmatrix} \quad (9)$$

where the subscripts indicate partial derivatives. The linear system in Eq. (8) has the following solution,

$$\begin{bmatrix} \delta \mathbf{r}(t) \\ \delta \mathbf{v}(t) \end{bmatrix} = \Phi(t, t_i) \begin{bmatrix} \delta \mathbf{r}(t_i) \\ \delta \mathbf{v}(t_i) \end{bmatrix} \quad (10)$$

$\Phi(t, t_i)$ is the 4×4 state transition matrix (STM) along the reference trajectory from t_i to t .

$$\Phi(t, t_i) = \begin{bmatrix} \Phi_{11}(t, t_i) & \Phi_{12}(t, t_i) \\ \Phi_{21}(t, t_i) & \Phi_{22}(t, t_i) \end{bmatrix} \quad \Phi(t_i, t_i) = I_4 \quad (11)$$

in which Φ_{ij} , ($i, j = 1, 2$) is the 2×2 submatrix of $\Phi(t, t_i)$ and I_4 is a 4×4 identity matrix.

According to the primer vector theory, the primer vector equation can be written in the first-order form as the linear system

$$\frac{d}{dt} \begin{bmatrix} \mathbf{p} \\ \dot{\mathbf{p}} \end{bmatrix} = \begin{bmatrix} 0 & I \\ \mathbf{G}_r & \mathbf{G}_v \end{bmatrix} \begin{bmatrix} \mathbf{p} \\ \dot{\mathbf{p}} \end{bmatrix} \quad (12)$$

The primer vector can then be evaluated along the transfer orbit using the state transition matrix $\Phi(t, t_i)$. Thus, the solution of the primer vector in the PBRFBP model is

$$\begin{bmatrix} \mathbf{p}(t) \\ \dot{\mathbf{p}}(t) \end{bmatrix} = \begin{bmatrix} \Phi_{11}(t, t_i) & \Phi_{12}(t, t_i) \\ \Phi_{21}(t, t_i) & \Phi_{22}(t, t_i) \end{bmatrix} \begin{bmatrix} \mathbf{p}(t_i) \\ \dot{\mathbf{p}}(t_i) \end{bmatrix} \quad (13)$$

The boundary conditions of the primer vector are defined as follows:

$$\mathbf{p}(t_i) \equiv \mathbf{p}_i = \frac{\Delta \mathbf{v}_i}{\|\Delta \mathbf{v}_i\|} \quad \mathbf{p}(t_f) \equiv \mathbf{p}_f = \frac{\Delta \mathbf{v}_f}{\|\Delta \mathbf{v}_f\|} \quad (14)$$

where, t_i, t_f are the initial and final time, respectively. $\dot{\mathbf{p}}(t_i)$ satisfies [22, 23]

$$\dot{\mathbf{p}}(t_i) = \Phi_{12}^{-1}(t_f, t_i)[\mathbf{p}(t_f) - \Phi_{11}(t_f, t_i)\mathbf{p}(t_i)] \quad (15)$$

provided $\Phi_{12}(t_f, t_i)$ is nonsingular. With both the primer vector $\mathbf{p}(t_i)$ and its first derivatives $\dot{\mathbf{p}}(t_i)$ known at the initial time $t = t_i$, the primer vector along the transfer trajectory for $[t_i, t_f]$ can be calculated by Eq. (13).

Lawden's necessary conditions for an optimal impulsive trajectory are [21]:

- 1. The primer vector and its first derivative must be continuous along the trajectory.
- 2. The magnitude of the primer vector $\|\mathbf{p}\|$ must be one at the instant of impulse and less than one elsewhere.
- 3. The primer vector is a unit vector in the optimal thrust direction at the impulse times.
- 4. The derivative $\dot{\mathbf{p}}$ must be zero at all interior impulses (except for the initial and final time). Meanwhile, the primer vector and its first derivative must be orthogonal at those times.

3 Problem statement

In this work, we investigate the three-impulse transfers from an initial circular Earth orbit of altitude $h_i = 167\text{km}$ to a final circular Moon orbit of altitude $h_f = 100\text{km}$ within 100 days in the PBRFBP model. The problem is defined as follows. At the initial time t_i , the first impulse of magnitude Δv_1 injects the spacecraft into a transfer trajectory. At the final time t_f ,

the final impulse of magnitude Δv_2 injects the spacecraft into the final Moon orbit. Let $\mathbf{x}_i = (x_i, y_i, \dot{x}_i, \dot{y}_i)$, $\mathbf{x}_f = (x_f, y_f, \dot{x}_f, \dot{y}_f)$ be the initial and final transfer state. The magnitudes of the initial and final maneuver are

$$\Delta v_1 = \sqrt{(\dot{x}_i - y_i)^2 + (\dot{y}_i + x_i + \mu)^2} - \sqrt{\frac{1 - \mu}{r_i}} \quad (16)$$

$$\Delta v_2 = \sqrt{(\dot{x}_f - y_f)^2 + (\dot{y}_f + x_f + \mu - 1)^2} - \sqrt{\frac{\mu}{r_f}} \quad (17)$$

where r_i is the scaled radius of the initial circular orbit about the Earth, and r_f is the scaled radius of the final circular orbit about the Moon. The boundary conditions are

$$\begin{aligned} (x_i + \mu)^2 + y_i^2 - r_i^2 &= 0 \\ (x_i + \mu)(\dot{x}_i - y_i) + y_i(\dot{y}_i + x_i + \mu) &= 0 \end{aligned} \quad (18)$$

$$\begin{aligned} (x_f + \mu - 1)^2 + y_f^2 - r_f^2 &= 0 \\ (x_f + \mu - 1)(\dot{x}_f - y_f) + y_f(\dot{y}_f + x_f + \mu - 1) &= 0 \end{aligned} \quad (19)$$

which means that the initial transfer state $\mathbf{x}_i = (x_i, y_i, \dot{x}_i, \dot{y}_i)$ is at a physical distance r_i from the Earth, and the final transfer state $\mathbf{x}_f = (x_f, y_f, \dot{x}_f, \dot{y}_f)$ is at a physical distance r_f from the Moon. The initial and final velocity vectors are aligned with the local circular velocity. Denote the left-hand sides Eq. (18) and Eq. (19) as $\psi(\mathbf{x}_i)$ and $\psi(\mathbf{x}_f)$, respectively. Then the boundary conditions are $\psi(\mathbf{x}_i) = 0$ and $\psi(\mathbf{x}_f) = 0$.

The two-impulse optimization problem satisfying the boundary conditions above has been solved by Topputo [12] through direct transcription and multiple shooting strategy. Therefore, the three-impulse optimization problem investigated in this work can be stated as follows: (1) to evaluate whether an additional interior impulse improves the performance of the previously obtained optimal two-impulse solutions. (2) If an additional impulse is needed, when and where the mid-course impulse $\Delta \mathbf{v}_m$ is implemented such that $\psi(\mathbf{x}_i) = 0$, $\psi(\mathbf{x}_f) = 0$, where the initial and the final time and positions, (t_i, x_i, y_i) and (t_f, x_f, y_f) are fixed, and the function

$$J = \|\Delta v_1\| + \|\Delta \mathbf{v}_m\| + \|\Delta v_2\| \quad (20)$$

is minimized.

4 Methodology

4.1 Criterion for an additional impulse

Considering a two-impulse reference trajectory Γ which transfers from the initial state \mathbf{x}_i at $t = t_i$ to the final

state \mathbf{x}_f at $t = t_f$. A neighboring perturbed trajectory Γ' with an addition mid-course impulse at t_m , and position $\mathbf{r}_m + \delta\mathbf{r}_m$ exists, in which \mathbf{r}_m is the position on Γ at $t = t_m$. Note that Γ' has the same terminal positions and times, (t_i, x_i, y_i) and (t_f, x_f, y_f) as Γ . Define the cost function of the reference trajectory Γ as J and the perturbed trajectory Γ' as J' . The cost function variation between Γ and Γ' is $\delta J = J' - J$. Based on the primer vector theory, the analysis in [22, 23, 28] show that

$$\delta J = c(1 - \mathbf{p}_m^T \hat{\boldsymbol{\eta}}) \quad (21)$$

where c is the magnitude of the mid-course impulse, \mathbf{p}_m is the primer vector at t_m on Γ and $\hat{\boldsymbol{\eta}}$ is an unit vector in the direction of the mid-course impulse. The variation $\delta J < 0$ indicates that the perturbed trajectory Γ' has a lower cost than the reference trajectory Γ . To make this happen, the numerical value of the dot product $(\mathbf{p}_m^T \hat{\boldsymbol{\eta}})$ in Eq. (21) should be greater than one at some time. Thus, it is necessary that $\|\mathbf{p}_m\| > 1$. The greatest decrease in the cost function is achieved only if the mid-course impulse is applied at the maximum of \mathbf{p}_m and in the direction of $\hat{\boldsymbol{\eta}}$. The position on the perturbed trajectory and the magnitude of the mid-course impulse are yet to be determined.

4.2 Calculation of the interior impulse

The calculation of the interior impulse begins with finding the position of the mid-course impulse. The position across the mid-course impulse is continuous. The state transition matrix before and after the mid-course impulse can be evaluated from $t_i \rightarrow t_m$ and from $t_f \rightarrow t_m$. Utilizing the information obtained from Eq. (21), The following variational equations of the position at $t = t_m$ are obtained.

$$\delta\mathbf{r}_m = cD^{-1} \frac{\mathbf{p}_m}{\|\mathbf{p}_m\|} \quad (22)$$

provided D is nonsingular. The expression of D is

$$D = \Phi_{22}(t_m, t_f)\Phi_{12}^{-1}(t_m, t_f) - \Phi_{22}(t_m, t_i)\Phi_{12}^{-1}(t_m, t_i) \quad (23)$$

To hold the assumption of the first-order perturbation theory, the magnitude of the mid-course impulse c should be selected as sufficiently small. The cost on the perturbed trajectory J' can be expressed as a function of c . The value of c can be estimated by minimizing J' . For example, Jezewski and Rozendaal [23] retain up to the second-order terms of the cost variation and obtain an analytical approximation of c in the two-body problem. Hiday [28, 29] minimized the algebraic expression $J'(c)$ by iteration method in the elliptic restricted three-body problem. In this work, following the method used by Hiday, the expression of J' as a function of c in

the PBRFBP model is

$$J' = (\Delta\mathbf{v}_0^T \Delta\mathbf{v}_0 + 2c\boldsymbol{\alpha}^T \Delta\mathbf{v}_0 + c^2\boldsymbol{\alpha}^T \boldsymbol{\alpha})^{\frac{1}{2}} + (\Delta\mathbf{v}_f^T \Delta\mathbf{v}_f - 2c\boldsymbol{\beta}^T \Delta\mathbf{v}_f + c^2\boldsymbol{\beta}^T \boldsymbol{\beta})^{\frac{1}{2}} + c \quad (24)$$

in which

$$\boldsymbol{\alpha} \triangleq \Phi_{12}^{-1}(t_m, t_i)D^{-1} \frac{\mathbf{p}_m}{\|\mathbf{p}_m\|} \quad \boldsymbol{\beta} \triangleq \Phi_{12}^{-1}(t_m, t_f)D^{-1} \frac{\mathbf{p}_m}{\|\mathbf{p}_m\|} \quad (25)$$

The magnitude of the mid-course impulse c is obtained by minimizing J' in Eq. (24). Thus, the position on Γ' at which the mid-course impulse should be applied is given by $\mathbf{r}_m' = \mathbf{r}_m + \delta\mathbf{r}_m$, in which \mathbf{r}_m is the position on Γ at $t = t_m$ and $\delta\mathbf{r}_m$ is given in Eq. (22).

4.3 Convergence to the optimal trajectory

Usually, adding the interior impulse does not necessarily produce an optimal three-impulse trajectory. Further optimization is needed by varying the time and position of the mid-course impulse. The variation in cost between the reference three-impulse trajectory Γ' and the perturbed three-impulse trajectory Γ'' are

$$\delta J' = \Delta\dot{\mathbf{p}}_m^T d\mathbf{r}_m + \Delta H_m dtm \quad (26)$$

where $\Delta\dot{\mathbf{p}}_m$ and ΔH_m are the primer vector and the Hamiltonian differences before and after the mid-course impulse, respectively. Both of them are determined on the reference three-impulse trajectory. The cost variation $\delta J'$ vanishes indicating that the trajectory is optimum. Therefore, the problem of determining an optimal trajectory becomes one of minimizing $J(\mathbf{r}_m, t_m)$ by a multivariable search method. Following previous works [29, 30], the Broydon-Fletcher-Goldfarb-Shanno(BFGS) variable metric method is utilized in this work.

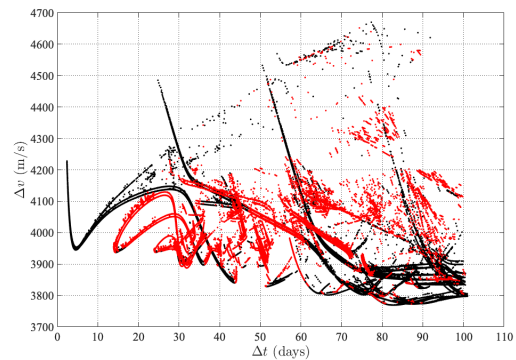


Fig. 1: Optimal two-impulse Earth-Moon transfer solutions obtained by Topputo [12], shown in the $(\Delta t, \Delta v)$ plane. The red color indicates the solutions to which a mid-course impulse can be added for further optimization.

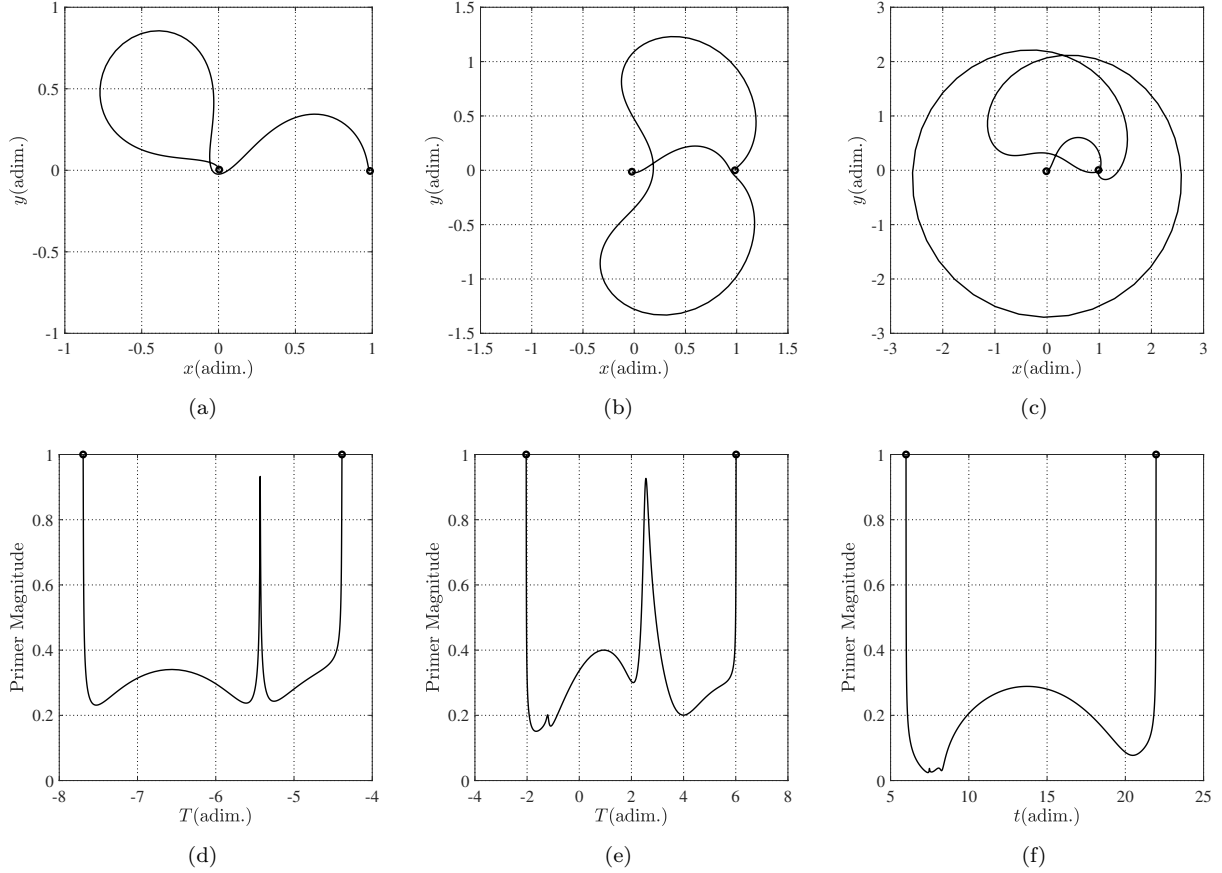


Fig. 2: Sample optimal two-impulse Earth-Moon transfers and their primer magnitude behaviors (no additional impulse required).

5 Results

The optimality of the two-impulse Earth-Moon transfers obtained by Topputo [12] is evaluated by computing the time history of the magnitude of the primer vector over the transfer duration of the trajectory. The global picture of optimal two-impulse Earth-Moon transfers is shown in the $(\Delta t, \Delta v)$ plane in Fig. 1. Each point in this figure is associated with an optimal two-impulse solution with transfer duration Δt and fuel cost Δv . Most of the two-impulse solutions obtained by Topputo meet the necessary conditions given by Lawden and no additional impulses are required for further optimization. These two-impulse solutions that satisfy Lawden's necessary conditions are indicated by black dots in Fig. 1. Three examples of the “no additional impulse required” optimal two-impulse trajectories and their primer magnitude behavior are shown in Fig. 2. The plot of the primer magnitude $\|p\|$ of the three example trajectories all satisfy the condition $\|p\| \leq 1$, and $\|p\| = 1$ only happens at the initial and final time. However, the evaluation results indicate that there are about a third of the

total solutions can be further optimized by adding an additional impulse (see the red dots in Fig. 1). Three example transfer trajectories and their primer magnitude are displayed in Fig. 3. The primer magnitude of the three example orbits exceeds unity. Therefore, the two-impulse transfer trajectories in Fig. 3 are not optimal and can be improved by adding a mid-course impulse. Denote the three example two-impulse transfer trajectories in Fig. 3 as case-1, case-2, and case-3, respectively. Further optimization of the three cases is executed. The first guess of the mid-course impulse locates where the primer magnitude attains its maximum (see the blue dots in Fig. 4). The position and time of the mid-course impulse are further optimized utilizing the method described in Sect. 4.3 until the gradient in Eq. (26) becomes trivially small. Finally, for each case, the transfer trajectories of the two-impulse as well as the optimal three-impulse and their primer magnitudes are presented together in Fig. 4.

The first example is case-1 in Fig. 3(a)(d). The magnitudes of initial and final impulse for the two-impulse transfer are 3.0661 km/s and 0.7911 km/s, respectively.

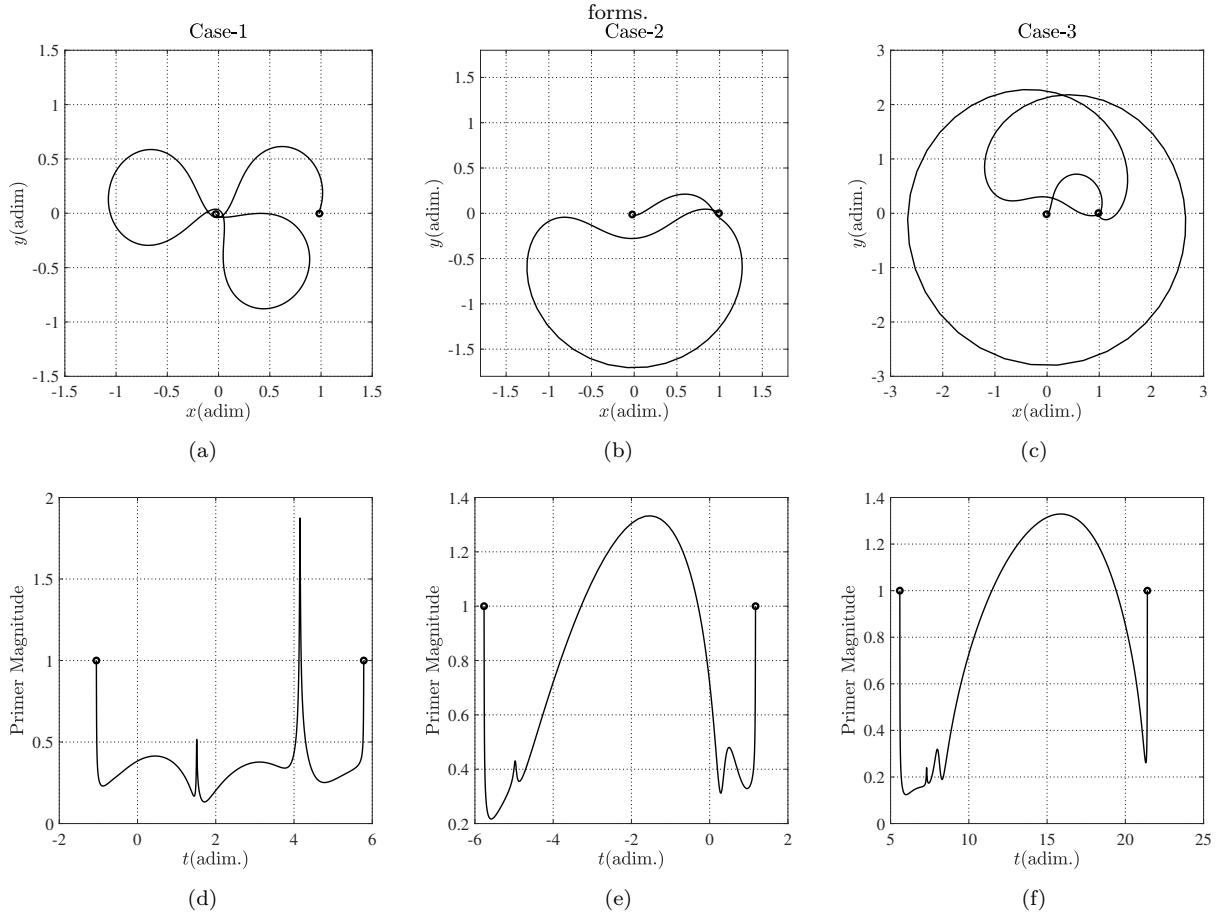


Fig. 3: Sample optimal two-impulse solutions and their primer magnitude behaviors (an additional impulse required).

The transfer duration is fixed at 29.7196 days. Utilizing the optimization process described above, the optimal three-impulse transfer is obtained. The velocity variation between the two-impulse transfer and the three-impulse transfer is nearly negligible ($\sim 10^{-9}$ km/s), implying that the current two-impulse solution is already near-optimal and the transfer trajectory is highly sensitive. For case-1, the two-impulse and three-impulse trajectories overlap (see Fig. 4(a)), but the primer magnitude behaviors are quite different (see Fig. 4(d)). The next example is case-2 in Fig. 3(b)(e). For the two-impulse transfer trajectory, the magnitudes of the two impulses are 3.0661 km/s (initial impulse) and 0.7690 km/s (final impulse). The time duration is fixed at 30.1726 days. The impulse magnitudes of the optimal three-impulse transfer trajectory are 3.0653 km/s (initial impulse), 0.0051 km/s (mid-course impulse) and 0.7633 km/s (final impulse). Compared with the two-impulse transfer, the cost of the optimal three-impulse decreases by 0.00137 km/s. The transfer trajectories and the primer magnitude corresponding to the two-impulse and the optimal three-impulse are presented in

Fig. 4(b) and Fig. 4(e). The transfer duration of case-3 (see Fig. 3(c)(f)) is 68.7795 days. The magnitudes of initial and final impulse for the two-impulse transfer are 3.0731 km/s and 0.6522 km/s, respectively. The velocity change between the two-impulse transfer and the three-impulse transfer is very small, about 10^{-7} km/s, indicating that the two-impulse transfer trajectory in case-3 is also highly sensitive and near-optimal. The overlap of the two-impulse and three-impulse trajectories are presented in Fig. 4(c) even if their primer magnitudes behave in different ways (see Fig. 4(f)).

6 Conclusion

This work focuses on the three-impulse, optimal low-energy Earth-Moon transfers in the planar bicircular restricted four-body problem. Based on the previously obtained two-impulse solutions, the optimization of the time-fixed three-impulse Earth-Moon transfer problem is further investigated with the primer vector theory and the BFGS algorithm. The cases studied in this work indicate that the primer vector cannot be considered as

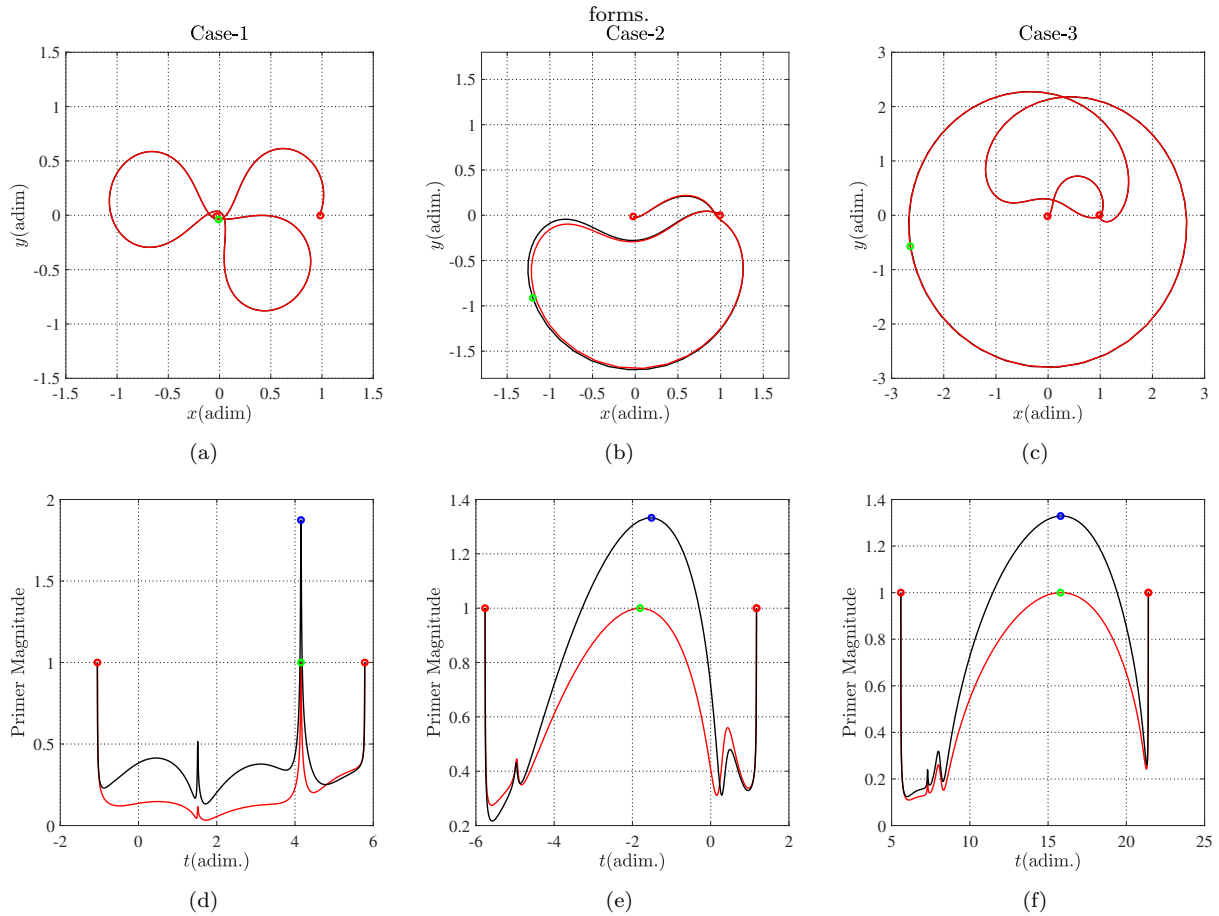


Fig. 4: The two-impulse (indicated by black color) and the optimal three-impulse (indicated by red color) Earth-Moon transfer trajectories and their primer magnitudes. The blue dots in (d-f) are the primer magnitudes that attain their maximum. The green dots are the positions of the mid-course impulses.

a representative of optimality in some situations, especially for the highly sensitive trajectory design problem. Subsequent work should consider the “mixed” algorithm (for example, the multiple shooting method combined with the BFGS method) to ease the computational difficulties due to the highly sensitive orbits. More results are being further calculated and a more general comparison between the two-impulse and three-impulse Earth-Moon transfers will appear in our future work.

Acknowledgments

This work is supported by the China Scholarship Council (No. 202006190153).

Bibliography

[1] E. Belbruno. Lunar capture orbits, a method of constructing earth moon trajectories and the lunar gas mission. *AIAA*, 06 1987.

[2] H. Yamakawa, J. Kawaguchi, N. Ishii, and H. Matsuo. On earth-moon transfer trajectory with gravitational capture. In *Advances in the Astronautical Sciences*, Advances in the Astronautical Sciences, pages 397–416, 1993.

[3] E. Belbruno and J. Miller. Sun-perturbed earth-to-moon transfer with ballistic capture. *Journal of Guidance Control and Dynamics*, 16, 09 1993.

[4] W.S. Koon, M.W. Lo, J.E. Marsden, and S.D. Ross. Shoot the moon. In *Advances in the Astronautical Sciences*, Spaceflight mechanics, pages 1017–1030, 2000.

[5] W.S. Koon, M.W. Lo, J.E. Marsden, and S.D. Ross. Low energy transfer to the moon. *Celestial Mechanics and Dynamical Astronomy*, 81, 09 2001.

[6] C. Circi and P. Teofilatto. On the dynamics of weak stability boundary lunar transfers. *Celestial Mechanics and Dynamical Astronomy*, 79:41–72, 01 2001.

- [7] E. Perozzi and A. Salvo. Novel spaceways for reaching the moon: An assessment for exploration. *Celestial Mechanics and Dynamical Astronomy*, 102:207–218, 09 2008.
- [8] G. Mingotti and F. Topputo. Ways to the moon: A survey. *Advances in the Astronautical Sciences*, 140:2531–2547, 01 2011.
- [9] J.S. Parker, R.L. Anderson, and A. Peterson. Surveying ballistic transfers to low lunar orbit. *Journal of Guidance, Control, and Dynamics*, 36(5):1501–1511, 2013.
- [10] J.S. Parker and R.L. Anderson. Targeting low-energy transfers to low lunar orbit. *Acta Astronautica*, 84:1–14, 03 2013.
- [11] H.L. Lei, B. Xu, and Y.S. Sun. Earth–moon low energy trajectory optimization in the real system. *Advances in Space Research*, 51:917–929, 03 2013.
- [12] F. Topputo. On optimal two-impulse earth–moon transfers in a four-body model. *Celestial Mechanics and Dynamical Astronomy*, 117, 11 2013.
- [13] R. Biesbroek and G. Janin. Ways to the moon? *ESA bulletin. Bulletin ASE. European Space Agency*, 103:92–99, 08 2000.
- [14] S. Hatch, M. Chung, J. Kangas, S. Long, R. Roncoli, and T. Sweetser. Trans-lunar cruise trajectory design of grail (gravity recovery and interior laboratory) mission. 08 2010.
- [15] K. Oshima, F. Topputo, and T. Yanao. Low-energy transfers to the moon with long transfer time. *Celestial Mechanics and Dynamical Astronomy*, 131, 01 2019.
- [16] K. Uesugi, H. Matsuo, J. Kawaguchi, and T. Hayashi. Japanese first double lunar swingby mission “hiten”. *Acta Astronautica*, 25:347–355, 07 1991.
- [17] K. Uesugi. Results of the muses-a “hiten” mission. *Advances in Space Research*, 18:69–72, 12 1996.
- [18] M.W. Lo, B. Williams, W. Bollman, D. Han, Y.S. Hahn, J. Bell, E. Hirst, R. Corwin, P. Hong, K.C. Howell, and et al. Genesis mission design. volume 49, 08 1998.
- [19] Tom Hoffman. Grail: gravity mapping the moon. pages 1–8, 04 2009.
- [20] R. Roncoli and K. Fujii. Mission design overview for the gravity recovery and interior laboratory (grail) mission. 08 2010.
- [21] D.E. Lawden. Optimal trajectories for space navigation. 01 1963.
- [22] P.M. Lion and M. Handelsman. Primer vector on fixed-time impulsive trajectories. *AIAA Journal*, 6:127–132, 02 1968.
- [23] D.J. Jezewski and H.L. Rozendaal. An efficient method for calculating optimal free-space n-impulse trajectories. *AIAA Journal*, 6, 12 1968.
- [24] J.E. Prussing. Optimal four-impulse fixed-time rendezvous in the vicinity of a circular orbit. *AIAA Journal*, 7, 06 1969.
- [25] J.E. Prussing. Optimal two- and three-impulse fixed-time rendezvous in the vicinity of a circular orbit. *Journal of Spacecraft and Rockets*, 40, 08 1970.
- [26] J.E. Prussing and J. Chiu. Optimal multiple-impulse time-fixed rendezvous between circular orbits. *Journal of Guidance Control Dynamics*, 9(1), 02 1986.
- [27] J.E. Prussing, L.J. Wellnitz, and W.G. Heckathorn. Optimal impulsive time-fixed direct-ascent interception. *Journal of Guidance, Control, and Dynamics*, 12(4):487–494, 08 1989.
- [28] L.A. Hiday-Johnston. *Optimal transfers between libration-point orbits in the elliptic restricted three-body problem*. PhD thesis, Purdue University, Indiana, September 1992.
- [29] L.A. Hiday-Johnston and K.C. Howell. Transfers between libration-point orbits in the elliptic restricted problem. *Celestial Mechanics and Dynamical Astronomy*, 58:317–337, 01 1994.
- [30] J. Guzman, L.M. Mailhe, C. Schiff, S. Hughes, and D. Folta. Primer vector optimization: Survey of theory, new analysis and applications. 02 2002.
- [31] K.A. Bokelmann and R.P. Russell. Optimization of Impulsive Europa Capture Trajectories using Primer Vector Theory. *Journal of the Astronautical Sciences*, 67(2):485–510, 05 2019.
- [32] D.J. Jezewski and N.L. Faust. Inequality constraints in primer-optimal, n-impulse solutions. *AIAA Journal*, 9, 05 1971.
- [33] D.J. Jezewski. Primer vector theory and applications. 12 1975.

- [34] D. Taur, C. Victoria, and J.E. Prussing. Optimal impulsive time-fixed orbital rendezvous and interception with path constraints. *Journal of Guidance, Control, and Dynamics*, 18(1):54–60, 1995.
- [35] Y.Z. Luo, J. Zhang, H.Y. Li, and G.J. Tang. Interactive optimization approach for optimal impulsive rendezvous using primer vector and evolutionary algorithms. *Acta Astronautica*, 67:396–405, 08 2010.
- [36] R. Serra, D. Arzelier, and A. Rondepierre. Analytical solutions for impulsive elliptic out-of-plane rendezvous problem via primer vector theory. *IEEE Transactions on Control Systems Technology*, PP:1–15, 02 2017.
- [37] L.A. D’Amario and T.N. Edelbaum. Minimum impulse three-body trajectories. *AIAA Journal*, 12, 02 1973.
- [38] K. Yagasaki. Sun-perturbed earth-to-moon transfers with low energy and moderate flight time. *celestial mech. dyn. astron.* 90, 197-212. *Celestial Mechanics and Dynamical Astronomy*, 90:197–212, 11 2004.
- [39] R.B. Negri and Antônio F. B. A. Prado. Generalizing the bicircular restricted four-body problem. *Journal of Guidance, Control, and Dynamics*, pages 1–7, 02 2020.
- [40] B.A. Conway. The problem of spacecraft trajectory optimization. *Spacecraft Trajectory Optimization*, pages 1–15, 01 2010.